Journal of the Korean Physical Society, Vol. 76, No. 9, May 2020, pp. 855∼859

A Solid-State Thin-Film Electrolyte, Lithium Silicon Oxynitride, Deposited by using RF Sputtering for Thin-Film Batteries

Dan Na, Byeongjun Lee, Baeksang Yoon and Inseok Seo*
School of Advanced Materials Engineering, Research Center for Advanced Materials Development (RCAMD), Chonbuk National University, Jeonju 54896, Korea

(Received 12 February 2020; revised 25 March 2020; accepted 13 April 2020)

In this study, a new lithium-silicon-oxynitride (LiSiON) solid-state thin-film electrolyte was investigated for the first time. The LiSiON thin-film electrolyte was deposited by using the RF sputtering technique. In order to compare the LiSiON thin-film electrolyte to lithium phosphorous oxynitride (LiPON), a conventional thin-film electrolyte, were deposited LiPON thin-film electrolytes by using RF sputtering. Surface morphologies and cross-sectional views of the thin-film electrolytes were characterized by using field emission scanning electron microscopy (FE-SEM). The thin-films showed smooth surfaces without any cracks and pinholes. The smooth surfaces are thought to decrease the interfacial resistance between the electrolyte and the electrodes. In addition, surface morphologies were characterized by using atomic force microscopy (AFM). The sputtering rates were calculated using the thicknesses of the thin-films, as obtained from cross-sectional views. The structural properties of the thin-films were characterized using X-ray diffraction (XRD). All thin-films showed amorphous properties compared to the target material which is a crystalline material. The ionic conductivity of the LiSiON thin-film was 2.47×10^{-6} (S/cm), which is slightly higher than that of a common thin-film electrolyte LiPON.

PACS numbers: 82.33.Pt, 81.15.Cd, 68.55.−a, 68.37.Hk, 61.05.cp
Keywords: Lithium silicon oxynitride, Thin-film electrolyte, Solid-state battery, Ionic conductivity, Amorphous
DOI: 10.3938/jkps.76.855

I. INTRODUCTION

At present, we are faced with various environmental issues, such as air pollution and rapid weather change. Air pollution is usually caused by the use of fossil fuels. Lithium-ion batteries (LIBs) are reasonable candidates for overcoming the environmental issues. These days, LIBs are very promising power suppliers for electronic devices, electrical vehicles (EVs), and energy storage systems (ESSs) because of their high power densities. Although LIBs have advantages compared to other power sources, LIBs with a liquid electrolyte have safety issues, such as the possibility of explosion and fire due to their thermal or chemical instability [1]. All solid-state batteries are the solution to the problem of LIBs with liquid electrolytes. All solid-state batteries have many advantages, such as the high energy densities and stabilities, and they can supply higher voltages than conventional LIBs can [2].

As portable and miniaturized electronic devices and the development of wearable types of batteries or devices are in the spotlight, the development of a power supply to drive them is indispensable. The type of battery that can meet this demand is an all-solid-state thin-film battery [3–5]. The thickness of a thin-film battery is about 10 μm, which makes it suitable for use as a power source in miniaturized electronic devices such as smart cards, RFID tags and medical devices [6]. All-solid-state thin-film batteries also have better thermal stability than conventional Li-ion batteries [2,7]. A higher capacity can be realized for thin-film batteries by applying high voltages [8]. The key to the performance of all-solid-state thin-film batteries is a solid electrolyte.

Various available techniques, such as a sputter [9], plasma laser deposition (PLD) [10], e-beam evaporator [11], and so on, can be used to deposit thin-film electrolytes. Among these techniques, the sputtering technique has an advantage compared to other deposition techniques. The sputtering techniques can be used to deposit oxide and nitride materials. In addition, sputtering techniques are simple and deposit thin-films uniformly. When compared to PLD and molecular-beam epitaxy (MBE), the sputtering techniques use a low temperature for deposition and are low cost. Therefore, the product of sputtering is suitable for commercialization.

Generally, solid electrolytes are classified as oxide or sulfide systems. While sulfide electrolytes have

*E-mail: isseo@jbnu.ac.kr

high ionic conductivity and low stability, oxide electrolytes have low ionic conductivity and high stability. Many oxide-based solid-state electrolytes have researched, including LiPON, $Li_7La_3Zr_2O_{12}$ (LLZO) [12], $Li_{1+x}Al_xTi_{2-x}(PO_4)_3$ (LATP) [13], and lithium boron oxynitride [14]. Among them, LiPON thin-film electrolytes are representative and commonly used as thin-film electrolytes. However, because the ionic conductivity of LiPON is relatively low, low ionic conductivity must be improved [12,13].

In this research, the LiSiON thin-film electrolytes were deposited using RF magnetron sputtering in an Ar/N_2 atmosphere. In order to compare the properties between LiSiON and LiPON thin-film electrolytes, we also deposited LiPON thin-films by using the same processes. Surface morphologies and cross-sectional views were investigated using field emission scanning electron microscopy (FE-SEM). The structural properties were analyzed using X-ray diffraction (XRD), and the ionic conductivities were evaluated using electrochemical impedance spectroscopy (EIS).

II. EXPERIMENTS AND DISCUSSION

1. Deposition of Thin-Films

In order to deposit thin-film electrolytes, we cleaned sapphire substrates with a thickness of 430 μm by using sonication in acetone and methanol and a rinse in 2-propanol. The substrates were dried using blowing N_2 gas. For the sputtering, the pressure of the vacuum chamber was less than 2.0×10^{-6} Torr. Pre-sputtering was carried out for 30 min to remove surface contamination on the sputtering target. Cu thin-films, which were to be used as blocking electrodes, with a 150 nm thickness were deposited by using direct-current (DC) magnetron sputtering with a 2-inch-diameter target. The DC power and the working pressure were set at 30 W and 7 mTorr in an Ar atmosphere, respectively. LiSiON and LiPON thin-films were deposited using RF magnetron sputter at 200 W power with 4 inch diameter Li_4SiO_4 and Li_3PO_4 targets, respectively in an Ar/N_2 (2:8) atmosphere.

In order to measure the ionic conductivities of the LiSiON and the LiPON thin-films, we deposited Cu/electrolyte/Cu overlap structures, as shown in Fig. 1, on a sapphire substrate. After sputtering, copper wires were attached onto Cu electrodes using silver paste.

2. Characterization of Thin-Film Electrolytes

Surface morphologies and cross-sectional views of LiSiON thin-films were evaluated by using FE-SEM (SU-70

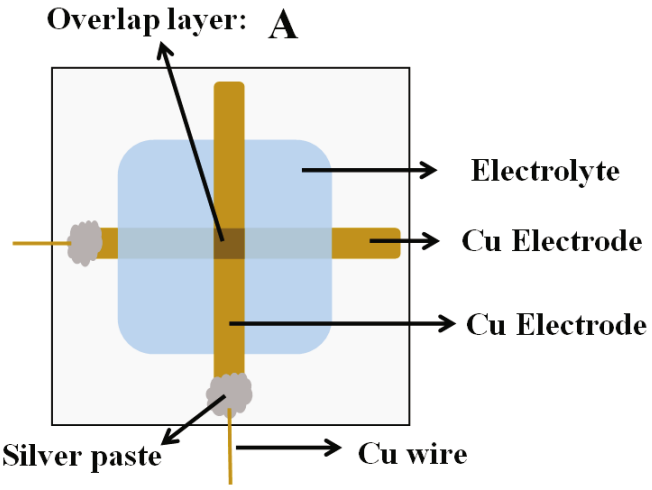

Fig. 1. Schematic structure for the EIS measurement sample.

HITACHI, Japan). The accelerating voltage for the FE-SEM measurements was set to 5 kV for surface images and 10kV for cross sectional images. The roughnesses of the thin-films were characterized using Atomic force microscopy (AFM, Bruker Multimode 8, USA). The images were taken in air at a 1-Hz scan rate and at resonance frequencies in the range of 840 – 860 kHz.

Structural properties of the thin-films were analyzed using XRD (MAX-2500 RIGAKU, Japan) with Cu-k_α radiation in the 2θ range of $20° \sim 80°$ with a step size of 0.05° and a scan rate of 1.0 deg/min. In addition, in order to compare the thin-films and the targets, we analyzed the powers of the targets. The ionic conductivity of the thin-film electrolytes was measured by using EIS (reference 3000 Gamry instruments, USA). Potentiostatic impedance spectroscopy was performed in the frequency range from 0.1 Hz to 1 MHz at room temperatures.

III. RESULTS AND DISCUSSION

Figures 2(a) and 2(b) show the FE-SEM surface morphologies of LiSiON and LiPON thin-films deposited as a solid electrolyte by using RF sputtering. Both thin-films showed smooth surfaces with neither cracks nor large particles. The smooth surfaces of the thin-films play an important role in improving the contact resistance between the electrolyte and the electrodes [15]. Cross-sectional views of the thin-films were also characterized by using FE-SEM, and the results are shown in Figs. 2(c) and 2(d). As shown in those figures, the thicknesses of the LiSiON and the LiPON thin-films were 464 nm and 430 nm for 120-min and 110-min depositions, respectively. The sputtering rates of the thin-films were calculated from their thicknesses. The sputtering rates of

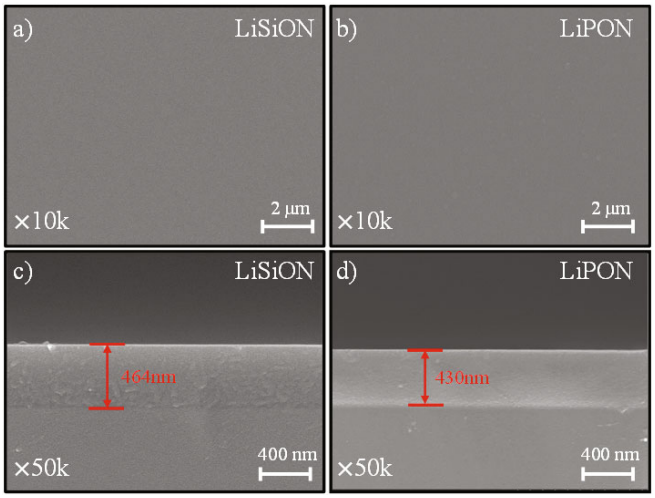

Fig. 2. Surface and cross-sectional FE-SEM images for LiSiON and LiPON thin films with the working pressure fixed at 3 mTorr.

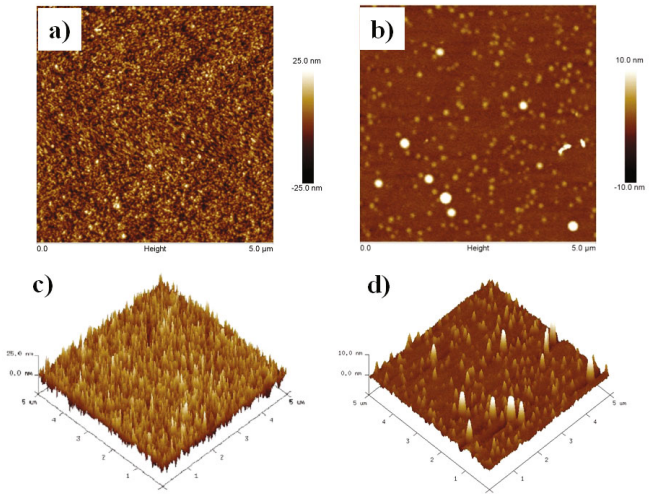

Fig. 3. AFM height images of (a) LiSiON thin films and (b)LiPON thin films and AFM 3D images of (c) LiSiON thin films, and (d) LiPON thin films in the contact mode. The size of each images is 5 μm × 5 μm.

the LiSiON and the LiPON thin-films were 3.87 nm/min. and 3.90 nm/min., respectively, which are very similar.

AFM was also applied to analyze the surface topographies of the LiSiON and the LiPON thin-films, and the results are shown in Fig. 3. Figures 3(a) and 3(b) show height images of the LiSiON and the LiPON thin-films, respectively, which Figs. 3(c) and 3(d) show 3D images of the LiSiON and the LiPON thin-films, respectively. The root-mean-squared (RMS) roughness of the LiSiON (5.452 nm) and the LiPON (6.015 nm) thin-films are observed to be similar. The RMS value for the LiSiON thin-film was slightly higher than that of the LiPON thin-film. Some obvious particles are observed on the LiPON thin-film (Fig. 3(d)). These results are very consistent with those from Fig. 2 and prove again the condition of the

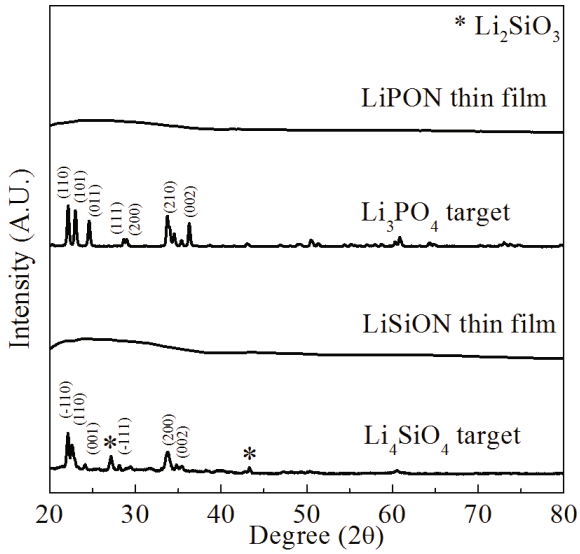

Fig. 4. XRD patterns for Li_4SiO_4 target, LiSiON thin film, Li_3PO_4 target, and LiPON thin film.

thin-films.

Figure 4 shows the XRD patterns of the Li_4SiO_4 target, LiSiON thin-film, Li_3PO_4 target, and LiPON thin-film. In order to analyze the XRD data for the two targets, we used Li_4SiO_4 and Li_3PO_4 the powders. For the XRD analysis, LiSiON and LiPON thin-films were deposited on sapphire substrates. As shown in Fig. 3, the XRD pattern of the Li_4SiO_4 target exhibit several peaks which were assigned at 22.2°, 22.6°, 24.1°, 28°, 33.7°, and 34.8° (Li_4SiO_4 - JCPDS 37-1472). Two peaks, one at 27.1° and the other at 43.2° were matched with the XRD pattern of Li_2SiO_3. Thus, while making the target using Li_2O and SiO_2 powders as starting materials, two crystalline phases, Li_4SiO_4 and Li_2SiO_3, may form and exist together if the starting powders are not well-mixed uniformly [16]. The XRD pattern of the Li_3PO_4 target show dominant peaks, which were assigned at 22.1°, 23.1°, 24.6°, 33.7° and 36.3° (Li_3PO_4 - JCPDS 25-1030). The XRD pattern of Li_3PO_4 did not show any peak related to other materials. Thus, the Li_3PO_4 target was homogeneous.

While the XRD patterns of the two targets showed several dominant peaks, which means a crystalline phase, the XRD patterns of the LiSiON and the LiPON thin-films did not show any dominant peaks. Thus, the crystalline Li_4SiO_4 and Li_3PO_4 targets appear to change into amorphous phases during sputtering. The reason an amorphous thin-film is deposited is that when the target material falls on the substrate quickly during RF sputtering, rapid quenching will occur [17]. Major factors of ion transport in inorganic ceramic composites are defects and electrostatic attraction and repulsion [18]. In the solid electrolyte, Lithium ions move by hopping between vacancies. Compared to a crystalline structure, generally an amorphous structure has more defects caused by its

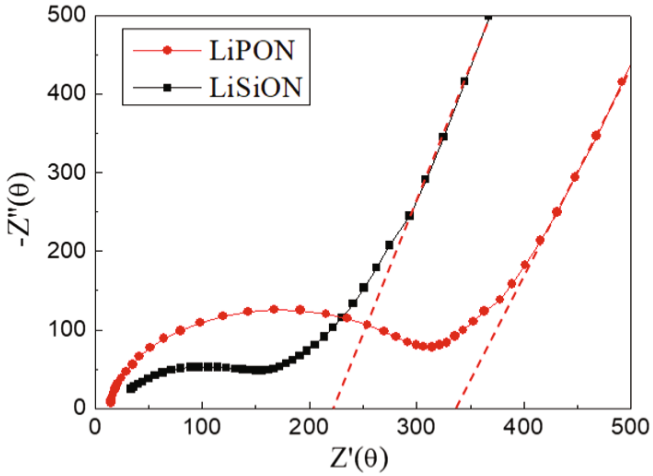

Fig. 5. Nyquist plots for the LiSiON and the LiPON thin-film electrolytes.

irregular arrangement. For this reason, these thin-films with amorphous structures may be better for transporting Li ions.

Figure 5 shows Nyquist plots for the LiSiON and the LiPON thin-films. These plots consist of semicircles in the high-frequency range and straight lines, which is due to the diffusion of ions between the electrolytes and the blocking electrodes, in the low-frequency range. From the Nyquist plot, the resistances of LiSiON and LiPON thin-films were found to be ∼220 Ω and ∼340 Ω, respectively. The ionic conductivity of the LiPON thin-film is 1.61×10^{-6} S/cm, which agrees very well with the reference values [19]. The ionic conductivity of the LiSiON thin-film is 2.47×10^{-6} S/cm, which is slightly higher than that of LiPON. As mentioned before, because the lithium ions have to pass through a glass network composed of positive and negative ions, they are disturbed by electrostatic attraction and repulsion. Thus, the ionic network and the chemical structure of the ceramic thin-film must be considered. Fleutot *et al.* investigated the chemical structure of LiPON thin-films [20]. A LiPON ceramic crystal, has bridging oxygen and nonbridging oxygen. LiPON, the nonbridging oxygens are in the forms of P=O and Li^+ ... -O-P. In bridging oxygens (O-P-O), P has two covalent bonds with oxygen. The lithium ion needs to move between these nonbridging oxygens, but the activation energy is determined by the size of the gap created by bridging oxygen. As a result of reactive sputtering with nitrogen, oxygen is replaced by nitrogen. This leads to a decrease in the ratio of the bridging oxygen to non-bridging oxygen, which affects the ionic conductivity of a LiPON thin-film. LiSiON is material for which the phosphorous sites in LiPON have been filled with silicon. Because they may have similar structure, they show similar ionic conductivities. The replacement of P by Si may change the bond length of the ions and the activation energy required for the hopping of Li ions. A change in the components in a glass network can affect the activation energy for the hopping of Li ions through a glass network [21] because mobile lithium ions, which hop through a glass network, undergo electrostatic interactions with the ions of glass components. Because the valence of Si (+4) is smaller than that of P (+5), Li ions are influenced by smaller electrostatic interactions, which can further improve the diffusivity of LiSiON. That's the reason the LiSiON thin-film has a slightly higher ionic conductivity than the LiPON thin-film.

IV. CONCLUSION

A new solid thin-film electrolyte, lithium silicon oxynitride (LiSiON), was successfully deposited on a sapphire substrate by using RF sputtering. In order to compare the properties of LiSiON thin-films with these of LiPON thin-films, we also deposited conventional solid thin-film electrolytes. The surface morphologies of LiSiON and LiPON thin-films were very similar and were without cracks or pin holes. In addition, surfaces of the two thin-film electrolytes, are analyzed using AFM, showed similar RMS values. Although the properties of the Li_4SiO_4 and the Li_3PO_4 targets indicated that those materials were crystalline, the properties of the two thin-film electrolytes indicated that those electrolytes were amorphous as a result of the sputtering. The ionic conductivity of a LiSiON thin-film was slightly higher than that of a LiPON thin-film. Therefore, LiSiON thin-film electrolytes are very promising materials for use in solid-state thin-film batteries. Further research on LiSiON thin-film electrolytes is needed before they can be applied to commercial products.

ACKNOWLEDGMENTS

This paper was supported by research funds for newly appointed professors of Jeonbuk National University in 2016. This work was also supported by National Research Foundation of Korea (NRF) (2017 R1A2B4007758) & (2018R1A4A1025528).

REFERENCES

[1] M. Armand and, J. M. Tarascon, Nature **451**, 652 (2008).
[2] Q. Wang *et al.*, J. Power Sources **208**, 210 (2012).
[3] D. Deng, Energy Sci. Eng. **3**, 385 (2015).
[4] H. Cha *et al.*, Small **14**, 1702989 (2018).
[5] K-H. Choi, D. B. Ahn and S-Y. Lee, ACS Energy Lett. **3**, 220 (2018).
[6] Y. Wang *et al.*, J. Power Sources **286**, 330 (2015).
[7] J. Schwenzel, V. Thangadurai and W. Weppner, J. Power Sources **154**, 232 (2006).

[8] J. Li *et al.*, Adv. Energy Mater. **5**, 1401408 (2015).
[9] K. F. Chiu *et al.*, Vacuum **84**, 1296 (2010).
[10] C. M. Julien and A. Mauger, Coatings **9**, 386 (2019).
[11] R. Z. Hu, M. Q. Zeng and M. Zhu, Electrochim. Acta **54**, 2843 (2009).
[12] D. J. Kalita *et al.*, Solid State Ion. **229**, 14 (2012).
[13] H. Chen, H. Tao, X. Zhao and Q. Wu, J. Non-Cryst. Solids **357**, 3267 (2011).
[14] S-W. Song, K-C. Lee and H-Y. Park, J. Power Sources **328**, 311 (2016).
[15] E. Crinon and J. T. Evans, Mater. Sci. Eng. A **242**, 121 (1998).
[16] P. C. Soares, E. D. Zanotto, V. M. Fokin and H. Jain, J. Non-Cryst. Solids **331**, 217 (2003).
[17] P. Duwez, R. H. Willens and W. Klement, Jr., J. Appl. Phys. **31**, 1136 (1960).
[18] S. W. Anwane, *Solid Electrolytes: Principles and Applications* (Wiley, Nagpur, 2014).
[19] J. Schwenzel, V. Thangadurai and W. Weppner, Ionics **9**, 348 (2003).
[20] B. Fleutot *et al.*, Solid State Ion. **186**, 29 (2011).
[21] Z. Gao *et al.*, Adv. Mater. **30**, 1705702 (2018).